MEASUREMENT OF SHALE GAS IN PLACE BASED ON DIFFERENT APPROACHES AND THEIR COMPARISON STUDY

by

Asadullah MEMON[a], Aifen LI[a*], Jie HU[a], Xiaoxia REN[a,b], Asif MEHMOOD[a], Qi FANG[a], Wencheng HAN[a], and Min MA[a]

[a] School of Petroleum Engineering, China University of Petroleum (East China), Qingdao, Shangdong Province, China
[b] School of Science, Qingdao University of Technology, Qingdao, Shangdong Province, China

Original scientific paper
https://doi.org/10.2298/TSCI190929467M

The understanding of gas sorption mechanism is essential to characterize the original gas-in-place for shale gas reservoirs. In this study, experimental data of five shale samples have been used to estimate the shale gas-in-place with new sights. Langmuir model is commonly used to measure the amount of adsorbed gas but this model does not include the amount of absorbed gas and its behavior. However, such gas usually contributes about 22% in respect to total gas storage even though its input remains undefined. Sorption model used in this study includes adsorbed and absorbed gas. Good results are obtained from sorption model as compared to Langmuir model. Variable range of total gas storage is observed using different approaches in all shale samples. Initially at low pressure, total gas storage is observed to be higher because of gas absorption contribution in new proposed approach when compared to approach-2. When pressure increases, total gas storage is altered in keeping with characteristics of adsorption and absorption of gas. Adsorbed and sorbed porosity is estimated at two different approaches and where total gas storages capacity is affected due to adsorbed or sorbed porosity. Further, the contribution of absorbed gas amount is found at about 19-22% in respect to total gas storage in all shale samples and that is in same range as mentioned in literature. The sorption model and new proposed approach includes adsorption and absorption of gases and provides new insights to understand the gas storage mechanisms and estimation of shale gas-in-place.

Key words: *free gas, adsorbed gas, absorbed gas, adsorbed porosity, sorbed porosity, gas-in-place*

Introduction

Shale gas reservoirs are unconventional reservoirs and are characterized by complex pore structure, low porosity, extremely low permeability, non-Darcy flow *etc*. [1, 2] and problems are consequently associated to assess the complexity of shale and predict the shale productivity [3, 4]. For shale gas reservoirs, the current volumetric methodologies are constructed on the basis of two volumes namely free and adsorbed gas volume. However, three forms of gas are present [5-7] in such reservoir *e. g*:

* Corresponding author, e-mail: aifenli@upc.edu.cn

– free gas which is stored in organic pore space and in natural fractures [8, 9] and this can be determined by amendments of standard reservoir evaluation approaches,
– adsorbed gas which is stored in organic matter *i. e*. kerogen and inorganic matrix *i. e.* clay mineral [8, 9] and this can be measured from the isotherm gas sorption measurements [10], and
– absorbed gas which is also stored in kerogen and associated with adsorbed gas.

The adsorbed and absorbed gas contributes in term of total gas storage about 20-80% [11] and 22% [12], respectively.

The absorbed gas remains associated with adsorbed gas but previous studies underestimated such gas in predicting the gas sorption and production behavior [13-16]. However, it is broadly recognized as gas dissolved into organic matter but has not yet attracted enough attention [17, 18].

Material balance is a common and excellent technique that is widely used in petroleum industry for estimation of original oil/gas in place in case when adequate field information is accessible. Nevertheless, in case adequate field information is not accessible. The volumetric methods can be practical. Generally, this method permits petroleum industry to measure the shale gas-in-place (GIP) with respect to the total gas by using key shale reservoir parameters that can be obtained through reservoir evaluation techniques such as well logging, coring, samples and well testing, *etc.* [5]. The understanding of shale complexity and accurate measurement of shale GIP is still a big question for petroleum industries and researchers beside the availability of advanced techniques and methods. Hence, keeping view on this question, sorption model (includes adsorbed and absorbed gas) has been proposed in this study to understand the gas storage mechanisms and estimate the shale GIP with new sights.

The following steps were followed to conduct this study: First, collected experimental data of five shale samples from literature [19]. Second, developed the sorption model by combining the adsorbed and absorbed gas equations. Third, measured the fitting parameters of models through fitting techniques and then compared the results of sorption model with Langmuir model. Fourth, measured the adsorbed and absorbed gas porosity based on sorption model; then, added adsorbed and absorbed gas porosity to measure the gas sorbed porosity. Fifth, measured the gas storage capacity at different approaches (*i. e.* two previous approaches and new proposed approach) and compared their results. At the end, investigated the effect of adsorbed and sorbed gas porosity on shale GIP by using different approaches and also measured the contribution of free, adsorbed and absorbed gases based on presented approaches.

Description of samples

Gas adsorption, bulk density, porosity and total organic carbon (TOC) data of five shale samples were taken from literature [19] to accomplish this study. The characteristics of five shale samples are shown in tab. 1.

Table 1. Characteristics of shale samples [19]

Shale sample	Bulk density [kgm^{-3}]	*TOC* [wt.%]	Porosity [%]	Kerogen type
A-1	2742	3.53	6.3	II
A-2	2502	9.20	7.1	I
A-3	2691	4.21	6.0	III
A-4	2674	5.10	6.5	I
A-5	2684	4.73	6.0	I

Models description and fitting parameters

Adsorption and absorption model

Langmuir model is the most common model and has widely been used to measure the absolute adsorption of gas [20]:

$$n_{\text{ads,ab}} = n_L \frac{P}{P_L + P} \tag{1}$$

where $n_{\text{ads,ab}}$ is the absolute adsorption capacity [mmolg/g], n_L – the langmuir volume [mmolg^{-1}], P and P_L – the equilibrium and Langmuir pressure [MPa]. Henry's law can be used to describe the absorbed gas [21]:

$$n_{\text{abs,ab}} = KP \times TOC \tag{2}$$

where $n_{\text{abs,ab}}$ is the molar number of absolute absorbed gas [mmolg^{-1}] and K is the Henry's law constant [mmol / (MPa g TOC)].

Sorption model

Combination of adsorption and absorption gas is known as sorbed gas. When combine eqs. (1) and (2), we can get eq. (3) which shows adsorption and absorption of gases:

$$n_{\text{sor,ab}} = n_L \frac{P}{P + P_L} + KP \times TOC \tag{3}$$

where $n_{\text{sor,ab}}$ is the molar number of absolute sorbed gas [mmolg^{-1}]. An excessive sorption can be obtained from the laboratory. Hence, conversion of excess to absolute sorption is necessary for estimation of shale GIP. Yu, *et al.* [16] provided a conversion of excess to absolute sorption by supposing the excess amount contains both adsorbed and absorbed gases:

$$n_{\text{sor,ex}} = n_{\text{sor,ab}} \left[1 - \left(\frac{k_{\text{ads}}}{\rho_{\text{ads}}} + \frac{k_{\text{abs}}}{\rho_{\text{abs}}} \right) \rho_{\text{gas}} \right] \tag{4}$$

where k_{ads} and k_{abs} [%] is the adsorption and absorption contribution in respect to total sorption, ρ_{gas}, ρ_{ads}, and ρ_{abs} [kgm^{-3}] is the free, adsorbed, and absored gas density.

It is worth noting that the density of adsorbed and absorbed gas phase is the key factor and plays a vital role in conversion of excess to absolute sorption. Previous studies assumed various density of adsorbed gas phase (ρ_{ads}) value in their studies. For example, Ambrose *et al.* [5] suggested ρads is around 0.34 g/cm^3. Yang [22] and Lei *et al.* [23] assumed 0.421 g/cm^3 adsorbed phase density for methane gas as the liquid density at boiling temperature and ambient pressure. Jing *et al.* [24] measured the adsorbed gas density ranges from 0.210-0.546 g/cm^3 and 0.209-0.489 g/cm^3 of six samples (shale and kerogen) based on Langmuir and SDR model by using least-square techniques at temperature 60 °C to 140 °C. Zhou *et al.* [25] presented three different techniques for measuring the adsorbed gas phase and concluded that DR gas adsorption model (excess) is a more reliable method than assuming liquid density (*i. e*. 0.373 g/cm^3 or 0.423 g/cm^3) or measure through linear relationship (gas adsorption *vs.* gas density).

As observed in the aforementioned literature studies that DR gas adsorption model (excess) is a more consistent method. Hence, this method used measurement of density of adsorbed gas phase in this study. The adsorbed gas phase density of all shale samples ranges from 0.304-0.339 g/cm^3 with an average value of 0.321 g/cm^3. For simplicity, the density of adsorbed gas phase was assumed 0.321 g/cm^3 while the density of kerogen was assumed 1.23 g/cm^3 in this study since ranges from 1.1 to 1.4 g/cm^3 for shale as observed in literature [26].

Curve fitting parameters of models

The curve fitting parameters of Langmuir and gas sorption models of all shale samples were obtained through curve fitting techniques and described in tab. 2. Equation (4) was used for conversion of excess to absolute sorption.

Table 2. Curve fitting parameters of models for all shale samples

Sample	Henry constant, K [mmol(MPag$_{TOC}$)$^{-1}$]	Langmuir model		Sorption model	
		n_L, [mmolg^{-1}]	P_L, [MPa]	n_L, [mmolg^{-1}]	P_L, [MPa]
A-1	0.05764	0.1064	1.380	0.08378	0.8975
A-2	0.06430	0.4072	2.567	0.3218	1.863
A-3	0.05182	0.1359	3.742	0.0991	2.579
A-4	0.05304	0.1490	2.463	0.1140	1.634
A-5	0.05125	0.1264	2.303	0.09376	1.492

Shale GIP estimation approaches

Approach-1

This is the old approach that used to estimate the total gas storage and includes volumes of free and adsorbed gas for total gas storage estimation [18, 27]:

$$G_t = G_f + G_{sorp} = \quad G_f + G_a \tag{5}$$

where G_t, G_f, and G_a are the total, free and adsorbed gas storage, respectively [scf/ton]. The volume of free gas can be measured:

$$G_f = 32.0368 \frac{\varphi\left(1 - S_{gi}\right)}{\rho_b B_g} \tag{6}$$

where φ and S_{gi} [%] is the initial porosity and gas saturation, ρ_b [gcm^{-3}] – the bulk rock density, and B_g – the gas formation volume factor. The volume of adsorbed gas can be estimate from Langmuir model as described in eq. (1).

Approach-2

This is the existing approach that has widely been used to estimate the total gas storage and includes volumes of free and adsorbed gas for total gas storage estimation. Ambrose *et al.* [5, 27] proposed a new method to estimate the total gas storage by correcting porosity, φ_a, before free gas volume estimation:

$$G_f = 32.0368 \frac{\varphi\left(1 - S_w\right) - \varphi_a}{\rho_b B_g} \tag{7}$$

where S_w is the initial water saturation.he porosity occupied by adsorbed gas can be expressed:

$$\varphi_a = 1.318 \cdot 10^{-6} M \frac{\rho_b}{\rho_s}\left(G_a\right) \tag{8}$$

where G_a [scf/ton] is adsorbed gas volume and can be measured from Langmuir model, ρ_s [gcm^{-3}] – the adsorbed gas phase density, and M [lb/lb$_{mol}$] – the molecular weight of natural gas. Further, adsorbed, absorbed or sorbed porosity can be measured:

$$\varphi_{\text{ads}} = \frac{n_{\text{ads,ab}} M_{\text{w}} \rho_{\text{b}}}{\rho_{\text{ads}}} \tag{9}$$

$$\varphi_{\text{abs}} = \frac{n_{\text{abs,ab}} M_{\text{w}} \rho_{\text{b}}}{\rho_{\text{abs}}} \tag{10}$$

$$\varphi_{\text{sor}} = \varphi_{\text{ads}} + \varphi_{\text{abs}} \tag{11}$$

Based on porosity correction, the eq. (7) may be re-written:

$$G_{\text{f}} = 32.0368\left[\left(\frac{\varphi(1-S_{\text{w}})}{\rho_{\text{b}}} - \frac{1.318\cdot 10^{-6} M}{\rho_{\text{s}}}\right)\left(n_L \frac{P}{P+P_L}\right)\right] \tag{12}$$

New proposed approach

In this approach, sorption model is to be used to estimate the total gas storage. Some modification of eq. (12) was undertaken based on sorption model for estimation of free gas volume:

$$G_{\text{f}} = 32.0368\left[\left(\frac{\varphi(1-S_{\text{w}})}{\rho_{\text{b}}} - \frac{1.318\cdot 10^{-6} M}{\rho_{\text{s}}}\right)\left(V_L \frac{P}{P+P_L} + KP \times TOC\right)\right] \tag{13}$$

Here, it is worth noting that free, adsorbed and absorbed volumes must be considered for total gas storage estimation as these volumes are present in shale gas reservoirs, therefore, the eq. (5) was also modified:

$$G_{\text{t}} = G_{\text{f}} + G_{\text{sorp}} = G_{\text{f}} + G_{\text{a}} + G_{\text{d}} \tag{14}$$

Further, as mentioned earlier that the Langmuir model does not contain the absorbed gas but on other hand, sorption model does contain both absorbed and adsorbed gas, hence; this approach may provide a new sight to accurate estimation of shale GIP.

Mechanism and parameters for shale GIP calculations

The composition of shale matrix, organic matter characteristics *i. e.* type, richness and maturity, structure of pores, pressure, temperature and water content are the main controlling factors that affect the physics and laws in shale gas storage [28, 29]. The mechanism of shale gas storage changes due to these controlling factors and resulted behavior of free, adsorbed and absorbed gas (total gas storage) is altered. Hence, it is essential to comprehend the mechanism

Table 3. Key reservoir parameters of five shale samples

Sample	A-1	A-2	A-3	A-4	A5
Porosity [%]	0.063	0.071	0.06	0.065	0.06
S_{w} [%] (assume)	0.35	0.35	0.35	0.35	0.35
S_{o} [%] (assume)	0	0	0	0	0
B_{g} (calculated)	0.01019	0.01019	0.010234	0.010234	0.029732
Molecular wt. [lb(lb_{mol})$^{-1}$]	16	16	16	16	16
Pressure [MPa]	10.2	10.2	10.16	10.16	10.16
Temperature [F]	158	158	158	158	158
Bulk rock density [gcm^{-3}]	2.742	2.502	2.691	2.674	2.684
Adsorbed gas phase density [gcm^{-3}] (assume)	0.321	0.321	0.321	0.321	0.321

of shale gas storage before calculation of shale GIP otherwise inaccuracy could be observed in the results.

The shale GIP can be calculated by using equations as mentioned in the section *Shale GIP estimation approaches* after getting the key shale reservoir parameters such as initial porosity, initial water and oil saturation, initial formation volume factor, bulk rock density and gas sorption through reservoir evaluation techniques. Table 3 describes the key reservoir parameters for shale sample that was used to measure the total gas storage at different approaches in this study.

Results and discussions

Gas sorption capacity

The Langmuir and gas sorption models were used to measure the gas sorption capacity of all shale samples. Figure 1 shows Langmuir model that includes only adsorbed gas and sorption model that includes both adsorbed and absorbed gas, hence it is observed that good results are obtained from sorption model as compared to Langmuir model and its value is also very close to experiments.

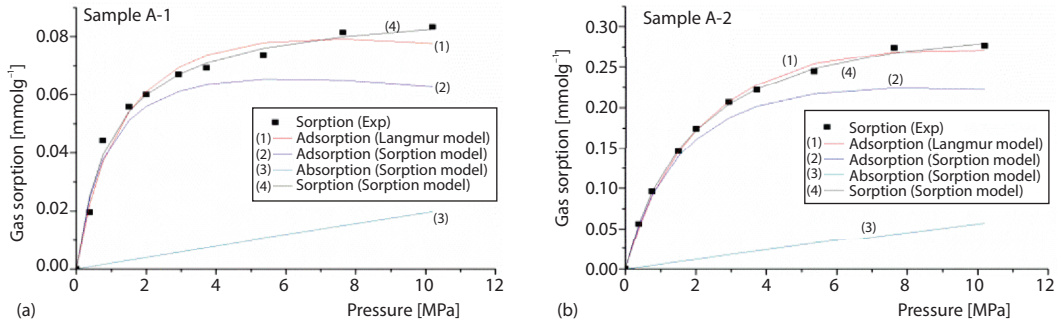

Figure 1. Gas sorption results based on Langmuir and sorption model for shale Samples A-1 and A-2

Shale GIP

The total gas storage capacities of all shale samples were measured using three different approaches as defined in section *Shale GIP estimation approaches*. Approach-1 is the old approach and does not correct volume occupied by adsorbed porosity in free gas volume estimation *e. g.* eq. (6). However, Approach-2 does correct for porosity volume occupied by adsorbed porosity in free gas volume estimation *e. g.* eq. (12) and the free and adsorbed gas volume was considered for total GIP estimation. However, this approach underestimates the amount of absorbed gas in shale GIP estimation. Sorption model includes both adsorbed and absorbed gas, this model has been used in new proposed approach *i. e.* eq. (13) and free, adsorbed and absorbed gas volumes were considered for total GIP estimation *i. e.* eq. (14). The calculated results of shale GIP of all samples based on aforementioned approaches are described in tab. 4-6.

From these tables, it was observed that when using the A-1 and A-2 for shale GIP estimation, the free, adsorbed and total gas storage capacities for shale sample A-1 represents a decrease of 31.26% and 12.44% of the free and total gas storage capacities, respectively. Similarly, shale samples A-2 to A-5 represent a decrease of 87.94%, 34.17%, 37.85%, and 35.36% of free and 16.72%, 12.84%, 13.32%, and 13.00% of total gas storage capacities, respectively.

Table 4. Shale GIP calculations based on Approach-1

Sample	A-1	A-2	A-3	A-4	A-5
G_f [scf/ton]	46.953	57.990	45.368	49.462	45.487
G_a [scf/ton]	71.067	247.923	75.384	91.025	78.210
G_t [scf/ton]	118.020	305.913	120.752	140.486	123.697

Table 5. Shale GIP calculations based on Approach 2

Sample	A-1	A-2	A-3	A-4	A-5
G_f [scf/ton]	32.275	9.991	29.866	30.742	29.403
G_a [scf/ton]	71.067	246.923	75.384	91.025	78.210
G_t [scf/ton]	103.341	253.934	105.250	121.767	107.612

Table 6. Shale GIP calculations based on new proposed approach

Sample	A-1	A-2	A-3	A-4	A-5
G_f [scf/ton]	31.628	5.876	29.572	29.843	28.881
G_a [scf/ton]	58.446	206.525	59.990	74.538	62.051
G_d [scf/ton]	15.752	45.797	16.823	20.860	18.693
G_t [scf/ton]	105.826	258.198	106.384	125.241	109.626

Further, observed that when using A-1 and new proposed approach, the free gas decreases on one end but the total gas storage increases on other end as compared to A-2. For example, sample A-1 to A-5 represents a decrease of 32.64%, 89.87%, 34.82%, 39.66%, and 36.51% of free and 10.33%, 15.32%, 11.90%, 10.85%, and 11.37% of total gas storage capacities, respectively. Furthermore, when using A-2 and new proposed approach that the free gas decreases while the total gas storage capacity increases might be due to contribution of gas absorption. For example, sample A-1 to A-5 represents a decrease of 2.00%, 15.95%, 0.98%, 2.92%, and 1.77% of free and an increase of 2.40%, 1.69%, 1.08%, 2.85%, and 1.87% of total gas storage capacities, respectively.

The average shale GIP calculated using the A-1, A-2, and new proposed approach was 161.574 scf/ton, 138.377 scf/ton, and 141.055 scf/ton, respectively. Here, it is worth noting that the average shale GIP calculated using new proposed approach is observed to be higher than A-2. Also, 2.485 scf/ton difference in total gas storage capacities was found in shale sample A-1 when using new proposed approach as compare to A-2 at pressure 10.2 MPa. Similarly, at same pressure, the 4.284 scf/ton, 1.135 scf/ton, 3.474 scf/ton, and 2.014 scf/ton difference in total gas storage capacities was also found in shale samples A-2 to A-5, respectively. Hence, these outcomes show that the absorbed gas must be accounted for accurate measurement of shale GIP for shale gas reservoirs.

The behavior of adsorbed, absorbed and total gas storage capacities with respect to pressure were also observed at various approaches for shale samples, figs. 2 and 3. Results show that initially at low pressure the total gas storage was higher due to contribution of absorbed gas when using new proposed approach as compared to A-2. When pressure increases, total gas storage was altered in keeping with characteristics of adsorption and absorption of gas. Even at same pressure, *i. e.* 10.2 MPa, the behavior of free, adsorbed and total gas storage capacity was observed to change may be due to different characteristics and properties of shale sample.

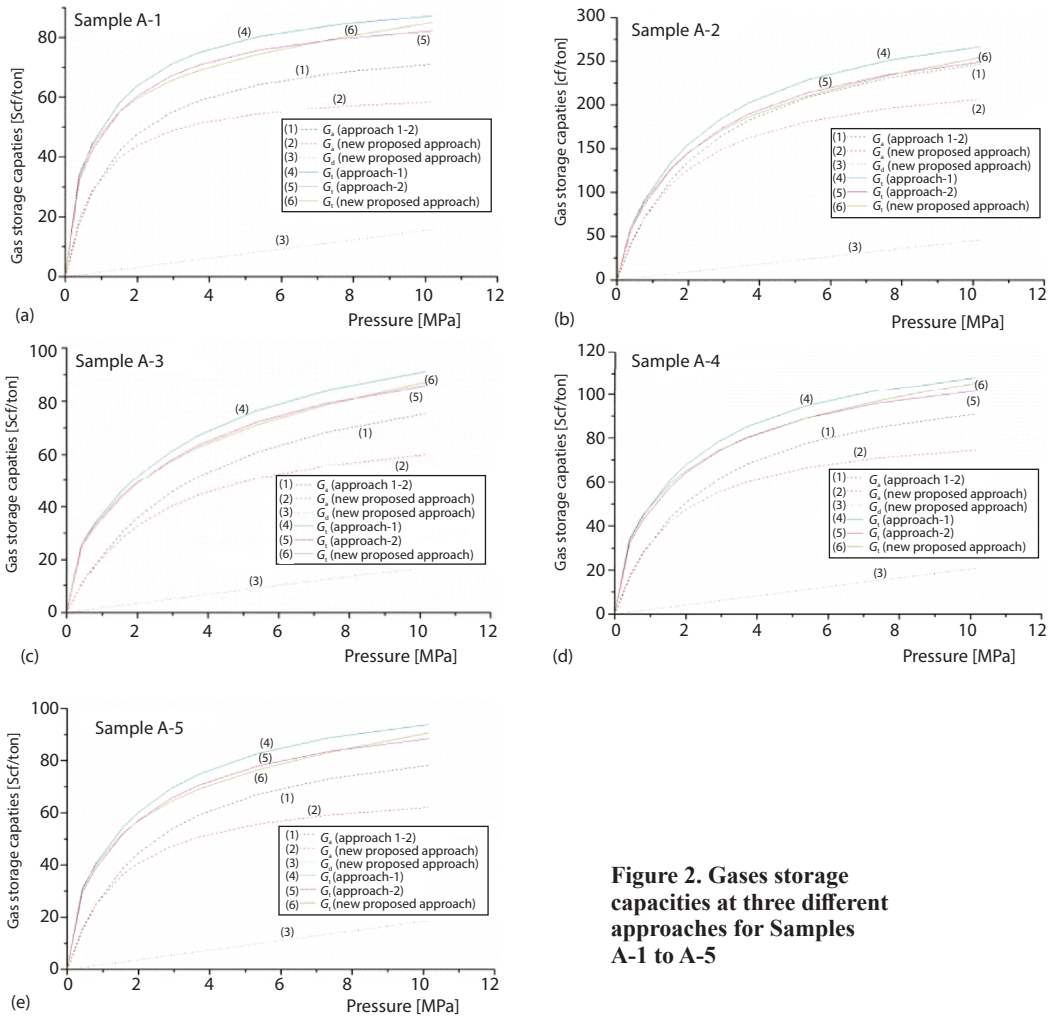

Figure 2. Gases storage capacities at three different approaches for Samples A-1 to A-5

Effect of adsorbed and sorbed gas porosity on shale GIP

The accurate measurement of adsorbed or sorbed porosity is playing an important role in accurate estimation of shale GIP as observed in literature. In this study, adsorbed or sorbed porosity was measured using A-2 and new proposed approach and results compared. The eq. (8) has commonly been used to measure the porosity occupied by adsorbed gas in A-2. However, the eqs. (9)-(11) can also be used to measure the adsorbed, absorbed and sorbed porosity. Table 7 describes the effect of adsorbed and sorbed porosity on shale GIP based on aforementioned approaches for all shale samples. It is observed from the results that adsorbed and sorbed porosity is creating some influences and changes in free gas volume and gas storage capacities.

Table. 7. Effect of adsorbed and sorbed gas porosity ontal gas storage for shale samples

Sample A-1						
Pressure [MP]	φ_a eq. (8)	G_t [scf/ton] eq. (5)	φ_a eq. (9)	G_t [scf/ton] eq. (14)	φ_s eq. (11)	G_t [scf/ton] eq. (14)
0.38	0.00314	32.279	0.00341	34.252	0.00344	34.241
0.76	0.00516	42.717	0.00526	44.354	0.00532	44.333
1.51	0.00759	55.263	0.00720	55.478	0.00731	55.435
2	0.00860	60.453	0.00792	59.960	0.00807	59.902
2.93	0.00989	67.058	0.00879	65.842	0.00900	65.758
3.73	0.0106	70.816	0.00925	69.472	0.00952	69.356
5.36	0.0115	75.712	0.00983	74.974	0.0102	74.820
7.63	0.0123	79.580	0.0103	80.735	0.0108	80.517
10.2	0.0128	82.128	0.0105	86.144	0.0112	86.853
Sample A-2						
Pressure [MPa]	φ_a eq. (8)	G_t [scf/ton] eq. (5)	φ_a eq. (9)	G_t [scf/ton] eq. (14)	φ_s eq. (11)	G_t [scf/ton] eq. (14)
0.38	0.00655	56.906	0.0068	60.025	0.0069	59.993
0.76	0.0116	85.478	0.0116	89.036	0.0118	88.973
1.51	0.0188	126.241	0.0180	128.241	0.0183	128.115
2	0.0222	146.641	0.0208	146.339	0.0212	146.172
2.93	0.0271	172.951	0.0246	171.748	0.0252	171.505
3.73	0.0301	189.989	0.0268	187.856	0.0275	187.646
5.36	0.0343	214.062	0.0298	212.332	0.0309	211.887
7.63	0.0380	234.765	0.0323	236.520	0.0338	235.886
10.2	0.0406	249.319	0.0340	257.647	0.0360	256.670
Sample A-3						
Pressure [MPa]	φ_a eq. (8)	G_t [scf/ton] eq. (5)	φ_a eq. (9)	G_t [scf/ton] eq. (14)	φ_s eq. (11)	G_t [scf/ton] eq. (14)
0.42	0.00184	25.288	0.00187	26.098	0.00190	26.085
0.81	0.00324	32.671	0.00318	33.660	0.00325	33.635
1.56	0.00536	43.817	0.00502	44.537	0.00514	44.490
2	0.00635	49.001	0.00582	49.450	0.00597	49.389
2.93	0.00801	57.707	0.00709	57.635	0.00731	57.545
3.73	0.00910	63.462	0.00788	63.107	0.00816	62.993
5.37	0.01075	72.102	0.0090	71.717	0.00941	71.552
7.36	0.01209	79.157	0.0099	79.551	0.0104	79.216
10.16	0.00133	85.664	0.0106	88.173	0.0114	87.862

→

Table 7. Continuation

Sample A-4						
Pressure [MPa]	φ_a [scf/ton] eq. (8)	G_t [scf/ton] eq. (5)	φ_a eq. (9)	G_t [scf/ton] eq. (14)	φ_s eq. (11)	G_t [scf/ton] eq. (14)
0.42	0.00290	32.334	0.00311	34.325	0.00315	34.310
0.81	0.00492	43.032	0.00505	45.331	0.00512	45.300
1.56	0.00770	57.774	0.00744	59.490	0.00759	59.431
2	0.00890	64.117	0.00838	65.373	0.00857	65.297
2.93	0.0108	74.118	0.00978	74.648	0.0101	74.537
3.73	0.0120	80.317	0.0106	80.583	0.0109	80.441
5.37	0.0136	89.068	0.0117	89.684	0.0122	89.480
7.36	0.0149	95.762	0.0125	97.919	0.0132	97.640
10.16	0.0160	101.606	0.0131	107.135	0.0141	106.750
Sample A-5						
Pressure [MPa]	φ_a eq. (8)	G_t [scf/ton] eq. (5)	φ_a eq. (9)	G_t [scf/ton] eq. (14)	φ_s eq. (11)	G_t [scf/ton] eq. (14)
0.42	0.00261	29.407	0.00276	30.953	0.00280	30.939
0.81	0.00440	38.853	0.00442	40.411	0.00449	40.384
1.56	0.00683	51.657	0.00642	52.321	0.00656	52.269
2	0.00786	57.091	0.00720	57.204	0.00737	57.136
2.93	0.00947	65.571	0.00833	64.856	0.00858	64.756
3.73	0.0104	70.773	0.00898	69.745	0.00930	69.679
5.37	0.0118	78.047	0.00984	77.277	0.0103	77.095
7.36	0.0129	83.557	0.0104	84.170	0.0111	83.921
10.16	0.0138	88.330	0.0110	92.001	0.0118	91.655

The contribution of free, adsorbed and absorbed gases was also observed on these approaches and found that the absorbed gas is contributing 19-22% in all shale samples as shown in tab. 8 and further noted that such contribution is the same in range as mentioned in literature.

Table 8. Contribution of free, adsorbed and absorbed gases for all shale samples

Shale sample	At pressure [MPa]	At Approach 2 based Langmuir model		At new proposed approach-based sorption model		
		Free gas [%]	Adsorbed gas [%]	Free gas [%]	Adsorbed gas [%]	Absorbed gas [%]
A-1	10.2	13.47	86.53	12.75	68.73	18.52
A-2	10.2	0.96	99.04	0.79	81.20	18.01
A-3	10.16	12.00	88.00	11.70	68.96	19.34
A-4	10.16	10.41	89.59	9.72	70.54	19.74
A-5	10.16	11.46	88.54	10.96	68.42	20.62

Conclusion

In this study, sorption model (includes adsorption and absorption of gas) provides better results as compared to Langmuir model. The underestimation of absorbed gas may affect the accurate estimation of shale GIP and understanding of shale gas behavior. The calculated shale GIP is based on three approaches including previous and new proposed approach and compared their results. In A-1 and new proposed approach, the free gas decreases more but on other end the total gas storage increases more as compare to A-1. And in A-2 and new proposed approach, the free gas decreases whereas the total gas storage capacity increases due to gas absorption effect. The behavior of adsorbed, absorbed and total gas storage capacities was also observed to differ at different pressures and this may due to adsorption and absorption characteristics of shale samples. It was also observed from this study that free gas volume and gas storage capacities was affected by adsorbed and sorbed porosity and the resulted change in shale GIP.

Acknowledgment

This work was supported by the National Natural Science Foundation of China |(No. 51774308) and the National Science and Technology Major Project of China (2016ZX05014-003-002).

Nomenclature

G_a – adsorbed gas storage, [scf/ton]
G_d – absorbed gas storage, [scf/ton]
G_f – free gas storage, [scf/ton]
G_t – total gas storage, [scf/ton]
K – Henry's law constant, [mmol(MPag$_{TOC}$)$^{-1}$]
M – molecular weight of natural gas, [lb/lb$_{mol}$]
P_L – Langmuir pressure, [MPa]
S_w – initial water saturation, [%]
V_L – Langmuir volume, [mmolg^{-1}]

Acronym

TOC – total organic carbon, [wt.%]

References

[1] Xu, J., *et al*., Production Performance Analysis for Composite Shale Gas Reservoir Considering Multiple Transport Mechanisms, *Journal Nat. Gas Sci. Eng.*, *26* (2015), Sept., pp. 382-395
[2] Liu, J., *et al.*, Flow Nonsistency between Non-Darcy Flow in Fracture Network and Non-Linear Diffusion in Matrix to Gas Production Rate in Fractured Shale Gas Reservoirs, *Transp. Porous Media*, *111* (2016), Oct., pp. 97-121
[3] Civan, F., Effective Correlation of Apparent Gas Permeability in Tight Porous Media, *Transp. Porous Media*, *82* (2010), 2, pp. 375-384
[4] Chaohua, G., *et al*., Improved Numerical Simulation for Shale Gas Reservoirs, *Proceedings*, Offshore Technology Conference-Asia, Kuala Lumpur, Malaysia, 2014
[5] Ambrose, R. J., *et al*., New Pore-Scale Considerations for Shale Gas in Place Calculations, *Proceedings*, SPE Unconventional Gas Conference Held, Pittsburgh, Penn., USA, 2010
[6] Sondergeld, C. H., *et al*., Micro-Structural Studies of Gas Shales, *Proceedings*, SPE Unconventional Gas Conference, Pittsburg, Penn., USA, 2010
[7] Lu, H.-J., *et al*., Mechanical Behavior Investigation of Long Maxi Shale under High Temperature and High Confining Pressure, *Thermal Science*, *23* (2019), 3A, pp. 1521-1527
[8] Yang, T., *et al*., Quantitative Dynamic Analysis of Gas Desorption Contribution Production in Shale Gas Reservoirs, *Journal Unconvent. Oil Gas Resour*, *9* (2015), 1, pp. 18-30
[9] Curtis, J. B., *Fractured Shale-Gas Systems*, AAPG Bulletin, Tulsa, Okla., USA, 2002, pp. 1921-1938
[10] Zhejun, P., Luke, D. C., Reservoir Simulation of Free and Adsorbed Gas Production from Shale, *Journal of Natural Gas Science and Engineering*, *22* (2015), Jan., pp. 359-370
[11] Wu, Y., *et al*., A Generalized Framework Model for the Simulation of Gas Production in Unconventional Gas Reservoirs, *SPE Journal*, *19* (2014), Jan., pp. 845-857
[12] Reza, E., *et al*., Measurement of Gas Storage Processes in Shale and of the Molecular Diffusion Coefficient in Kerogen, *Int. J. Coal Geol.*, *123* (2014), Mar., pp. 10-19

[13] Weichao, Y., *et al*., A Novel Method for Estimation of Remaining Oil Saturations in Water-Flooded Layers, *Interpretation*, *5* (2017), 1, pp. 9-23
[14] Yan,W., *et al*., Arobust NMR Method to Measure Porosity of Low Porosity Rocks, *Microporous Mesoporous Mater*, *269* (2018), Oct., pp. 113-117
[15] Golsanami, N., *et al*., Distinguishing Fractures from Matrix Pores Based on the Practical Application of Rock Physics Inversion and NMR Data: A Case Study from an Unconventional Coal Reservoir in China, *Journal Nat. Gas Sci. Eng*., *65* (2019), May, pp. 145-167
[16] Yu, P., *et al*., Experimental Measurement and Analytical Estimation of Methane Absorption in Shale Kerogen, *Fuel*, *240* (2019), Mar., pp. 192-205
[17] Jixiang, H., *et al*., A Quadruple-Porosity Model for Shale Gas Reservoirs with Multiple Migration Mechanisms, *Journal of Natural Gas Science and Engineering*, *33* (2016), July, pp. 918-933
[18] Wei, Y., *et al.*, Evaluation of Gas Adsorption in Marcellus Shale, *Proceedings*, SPE Annual Technical Conference and Exhibition held in Amsterdam, Amsterdam, The Netherlands, 2014
[19] Pang, Y., *et al*., Effect of Methane Adsorption on Stress-Dependent Porosity and Permeability in Shale Gas Reservoirs, *Proceedings*, SPE Low Perm Symposium, Denver, Col., USA, 2016
[20] Xue, Y., *et al*., Effect of Damage on Gas Seepage Mechanism in Coal Seam Based on a Coupled Model, *Thermal Science*, *23* (2019), 3A, pp. 1323-1328
[21] Xiukun, W., James, S., Gas Sorption and Non-Darcy Flow in Shale Reservoirs, *Petroleum Science*, *14* (2017), 1, pp. 746-754
[22] Yang, F., *et al*., Investigations on the Methane Sorption Capacity of Marine Shales from Sichuan Basin, China, *International Journal of Coal Geology*, *146* (2015), July, pp. 104-117
[23] Lei, C., *et al*., Mechanisms of Shale Gas Adsorption: Evidence from Thermodynamics and Kinetics Study of Methane Adsorption on Shale, *Chemical Engineering Journal*, *361* (2019), Apr., pp. 559-570
[24] Jing, L., *et al*., Characterization of Methane Adsorption on Shale and Isolated Kerogen from the Sichuan Basin under Pressure up to 60 MPa: Experimental Results and Geological Implications, *International Journal of Coal Geology*, *189* (2018), Mar., pp. 83-93
[25] Shangwen, Z., *et al*., Experimental Study of Supercritical Methane Adsorption in Longmaxi Shale: Insights into the Density of Adsorbed Methane, *Fuel*, *211* (2018), Jan., pp. 140-148
[26] Yu, P., *et al*., Experimental Measurement and Analytical Estimation of Methane Absorption in Shale Kerogen, *Fuel*, *240* (2019), Mar., pp. 192-205
[27] Ambrose, R. J., *et al*., Multi-Component Sorbed-Phase Considerations for Shale Gas-in-Place Calculations, SPE Production Operations Symposium held in Oklahoma City, Okla., USA, 2011
[28] Fang, H., *et al*., Mechanisms of Shale Gas Storage: Implications for Shale Gas Exploration in China, *AAPG Bulletin*, *97* (2013), 8, pp. 1325-1346
[29] Yan, W., *et al*., A Robust NMR Method to Measure Porosity of Low Porosity Rocks, *Microporous Mesoporous Mater*, *269* (2018), Oct., pp. 113-117

Paper submitted: September 29, 2019
Paper revised: December 16, 2019
Paper accepted: December 27, 2019